CBN 96-2
D.Rubin
February 28, 1996

Optical Effects of Parasitic Crossings with Nine Trains of Bunches

Introduction

In a colliding beam machine with a single ring and n bunches/beam, there are $2n-1$ parasitic crossings of the counterrotating bunches. The guide field of one beam depends on the charge per bunch in the opposing beam via the long range interaction at each of the parasitic crossing points. In the CESR crossing angle configuration there are nine trains of two to five bunches in each beam. The bunches within each train are either 14ns or 28ns apart. We find that the closed orbits, the betatron tunes, beta-functions and chromaticities of one beam are distorted as a result of the multiple long range interactions. The details of the distortion depend on the transverse separation of the bunches, and the betatron functions at each of the crossing points.

The bunches in each beam are not evenly spaced about the circumference of the machine. Therefore each bunch in one beam will interact with the bunches in the counterrotating beam at a bunch dependent combination of locations around the ring. The β-functions and the separation of the closed orbits varies from one crossing point to the next. Because of the uneven spacing, the distortion of optical functions and closed orbits is not the same for all of the bunches. The combined effect of all of the long range interactions is bunch specific. The bunch and current dependence of the tunes, β_h^* and β_v^*, the crossing angle, and the chromaticities are computed for various configurations of bunches.

The Model

The long range beam-beam kicks are incorporated into a model of the CESR lattice that includes design quadrupoles and sextupoles, CLEO experimental

solenoid and rotated IR quad compensation, and the four horizontal and two vertical separator kicks. A beam-beam kick is added at each of the parasitic crossing points. The location of the kicks depends on the number of bunch trains and the spacing of the trains, and the number of bunches per train and spacing within the train.

Long range beam-beam kick

A line charge approximation is used to characterize the long range beam-beam interaction. The charge distribution is gaussian but because the beams are always separated by at least several horizontal beam sizes, the line charge approximation is appropriate. In particular if $\mathbf{\Delta x}'_-$ is the kick experienced by an electron in the field of the stored positron beam then,

$$\mathbf{\Delta x}'_- = 2r_0 N \frac{\mathbf{x}_+ - \mathbf{x}_-}{\gamma |\mathbf{x}_+ - \mathbf{x}_-|^2}. \tag{1}$$

r_0 is the classical electron radius, N the number of particles in the positron bunch, and $\mathbf{x}_+$ the transverse coordinates of the positron closed orbit and $\mathbf{x}_-$ the coordinate of the electron at the crossing point. Note that the effective dipole kick scales inversely with the separation, the quadrupole kick inversely with the square of the separation, etc. The long range kick is always horizontally defocusing and vertically focusing for horizontally separated, oppositely charged beams. The effective focal length is given by

$$\frac{\mathbf{\Delta x}'_-}{\mathbf{\Delta x}_-} = 2r_0 N \frac{1}{\gamma |\mathbf{x}_+ - \mathbf{x}_-|^2} = \frac{1}{f} \tag{2}$$

Now $\mathbf{x}_-$ refers to the coordinate of the closed orbit of the electron beam and $\mathbf{\Delta x}_-$ displacement with respect to the closed orbit. The tune shift is

$$\Delta Q = \frac{\beta}{4\pi f} = r_0 N \frac{\beta}{2\pi\gamma |\mathbf{x}_+ - \mathbf{x}_-|^2} \tag{3}$$

The beam-beam kick can also be treated more generally, as due to a two-dimensional gaussian charge distribution that depends on local beam size. As shown below, the line charge approximation turns out to be a good one.

Procedure

The procedure for determining the effect of the parasitic kicks is to first compute the closed orbit (including separator kicks) of the strong beam. Then a single bunch in the counterrotating beam is introduced in a weak strong scenario where we assume no effect of weak beam on strong beam. At each of the parasitic crossings witnessed by the particular weak beam bunch, the position of the weak beam with respect to the closed orbit of the strong beam yields the beam-beam kick. The closed orbit and transfer map of the weak beam is derived from the computed change in the phase space coordinates in a single turn. The beam-beam kick at the interaction point is not included.

Train and bunch spacing

Spacing of the trains around the circumference of the ring is not uniform. During Phase I bunch train operation, the spacing of the nine trains was relatively uneven. There were 280ns between train 1 and 2, 280ns between train 2 and 3, ... , and 280ns between train 8 and 9. Then there were 322ns between train 9 and 1. The two bunches within each train were spaced 28ns apart. The electron and positron closed orbits and the parasitic crossing points are shown in Figure 1. There is a unique set of parasitic crossings for each bunch.

In Phase II operation, the nine trains are spaced somewhat more evenly around the ring. There are 280ns between train 1 and 2, 280ns between train 2 and 3, and 294ns between train 3 and 4. Then the pattern repeats so that there are 280ns between train 4 and 5, 280ns between 5 and 6 and 294ns between 6 and 7. Finally there are 280ns between trains 7 and 8, 280ns between 8 and 9 and 294 between 9 and 1. The closed orbits and parasitic crossings for trains with two bunches spaced 28ns apart are shown in Figure 2. Note that in Phase I the parasitic crossings fill a slightly larger fraction of the machine circumference than in Phase II due to the more uneven train spacing. As a result, in Phase II there tend to be fewer parasitic crossings far from the pretzel maxima than in Phase I.

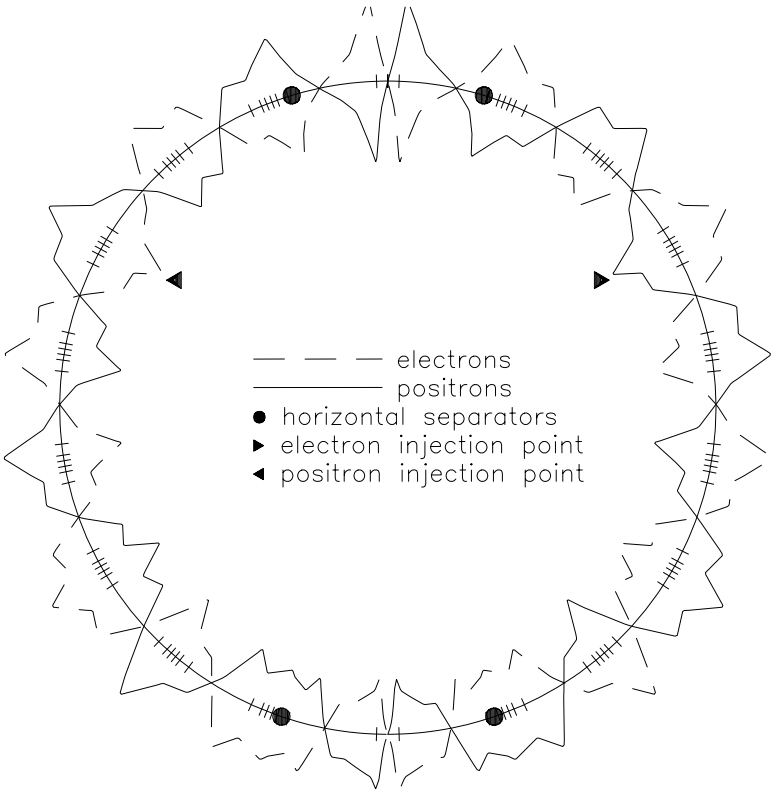

Figure 1: Closed orbits for electrons and positrons and all parasitic crossing points are indicated for the Phase I "uneven" spacing. Note that each of the 18 bunches in one beam encounter a near miss with the opposite beam at a unique set of 35 of the crossing points.

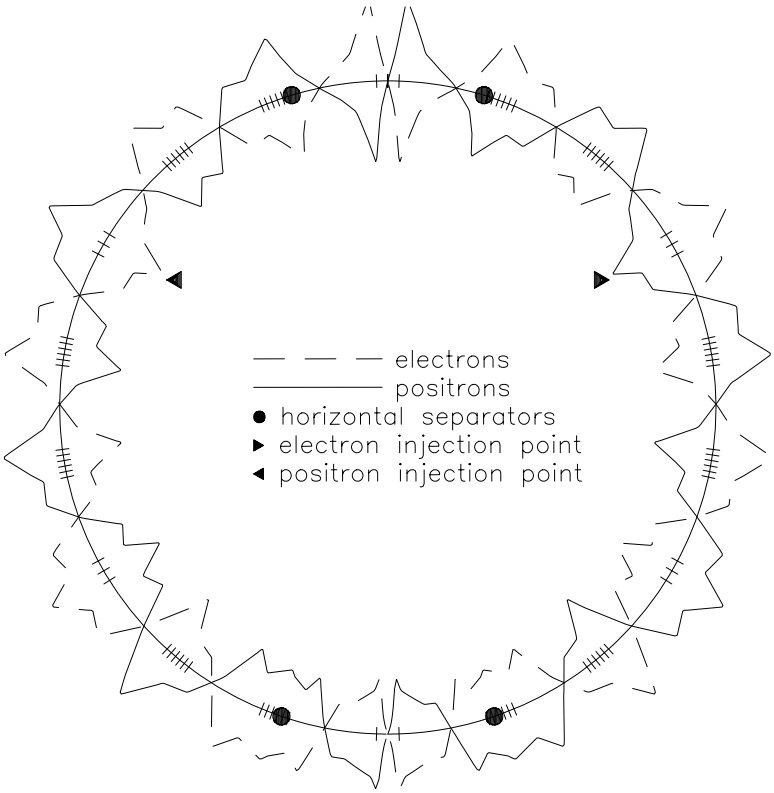

Figure 2: Closed orbits for electrons and positrons and all parasitic crossing points are indicated for the Phase II "even" train spacing. Note that each of the 18 bunches in one beam encounter a near miss with the opposite beam at a set of only 35 of the crossing points. Trains 1,4 and 7 share the same set of parasitic crossing points, as do trains 2,5,8 and trains 3,6,9.

Results

The current dependence of the weak beam bunch #1 closed orbit, tunes, β-functions and chromaticities is computed as a function of the current in the strong beam. Then for a fixed strong beam bunch current of 10mA/bunch, the optical functions are computed for each of the weak beam bunches. The crossing angle is $\pm$2.3mrad and the vertical separator kick is $\pm$1mrad The results are shown for a variety of configurations.

The current and bunch dependence of optical functions is computed for the Phase I on resonance optics N9A18A600.FD92S_4S with 9 2-bunch trains. The trains are distributed according to the "uneven" Phase I spacing described above and the bunches within each train are 28ns apart. The beam-beam kicks are based on the line charge approximation. The results are shown in Figure 3 and Figure 4

We see from Figure 3 that horizontal tune falls with increasing current in the opposing beam. This is consistent with our experience during electron injection. As the electron current increases the horizontal tune of the positrons decreases. In practice, the positron tune is initially just above a synchrotron side-band and the falling tune is manifested as deteriorating lifetime and increasing radiation. In order to preserve the positrons it is necessary to increase the horizontal tune.

The vertical β-function at the interaction point is very nearly independent of current in the strong beam while the horizontal β^* suffers a 25% reduction with 10ma/bunch of positrons. This is presumably due to the fact that the parasitic crossings are all nearly 180° apart in horizontal betatron phase and add coherently. The vertical phase relationship is more nearly random. Also, the proximity to the horizontal half integer tune magnifies the effect of the quadrupole errors on the horizontal β-function.

The dependence of crossing angle of the weak beam on current in the strong beam characterizes the distortion of the closed orbit around the ring. We see that the crossing angle, (and presumably the closed orbit in general), changes by about 10% with 10ma/bunch in the opposing beam. The change in vertical displacement at the IP is due to the parasitic crossing at the L3 symmetry point where the beams are vertically separated.

The variation in tune from one weak beam bunch to the next is shown in Figure 4(a). There is very little bunch dependence of the horizontal tune and dependence of the vertical tune is limited to a range of of 2kHz. Note

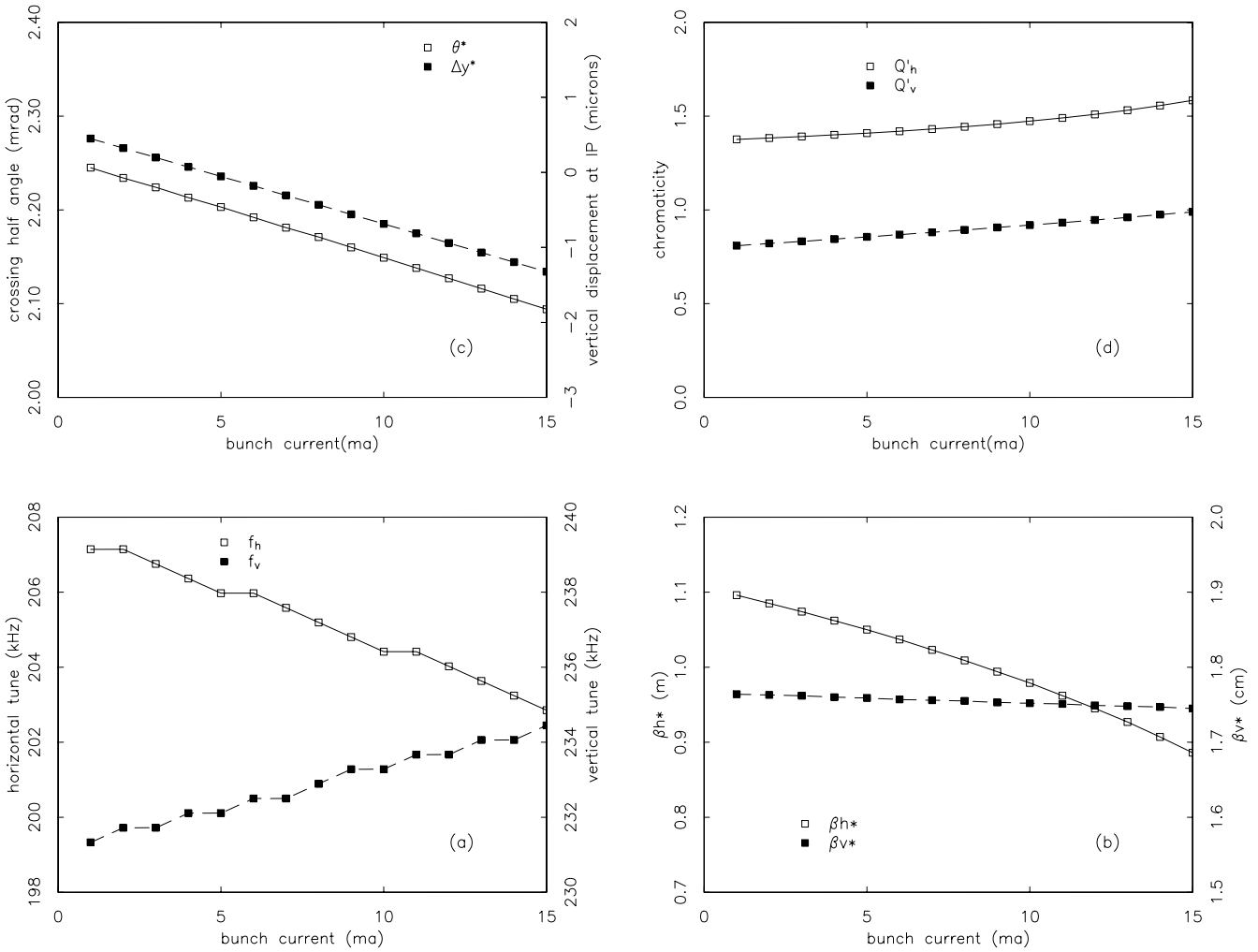

Figure 3: Horizontal and vertical tune of weak beam bunch #1 (a) as a function of positron bunch current for 18 bunches of positrons, β^* in (b), horizontal crossing angle and vertical displacement in (c), and chromaticity in (d).

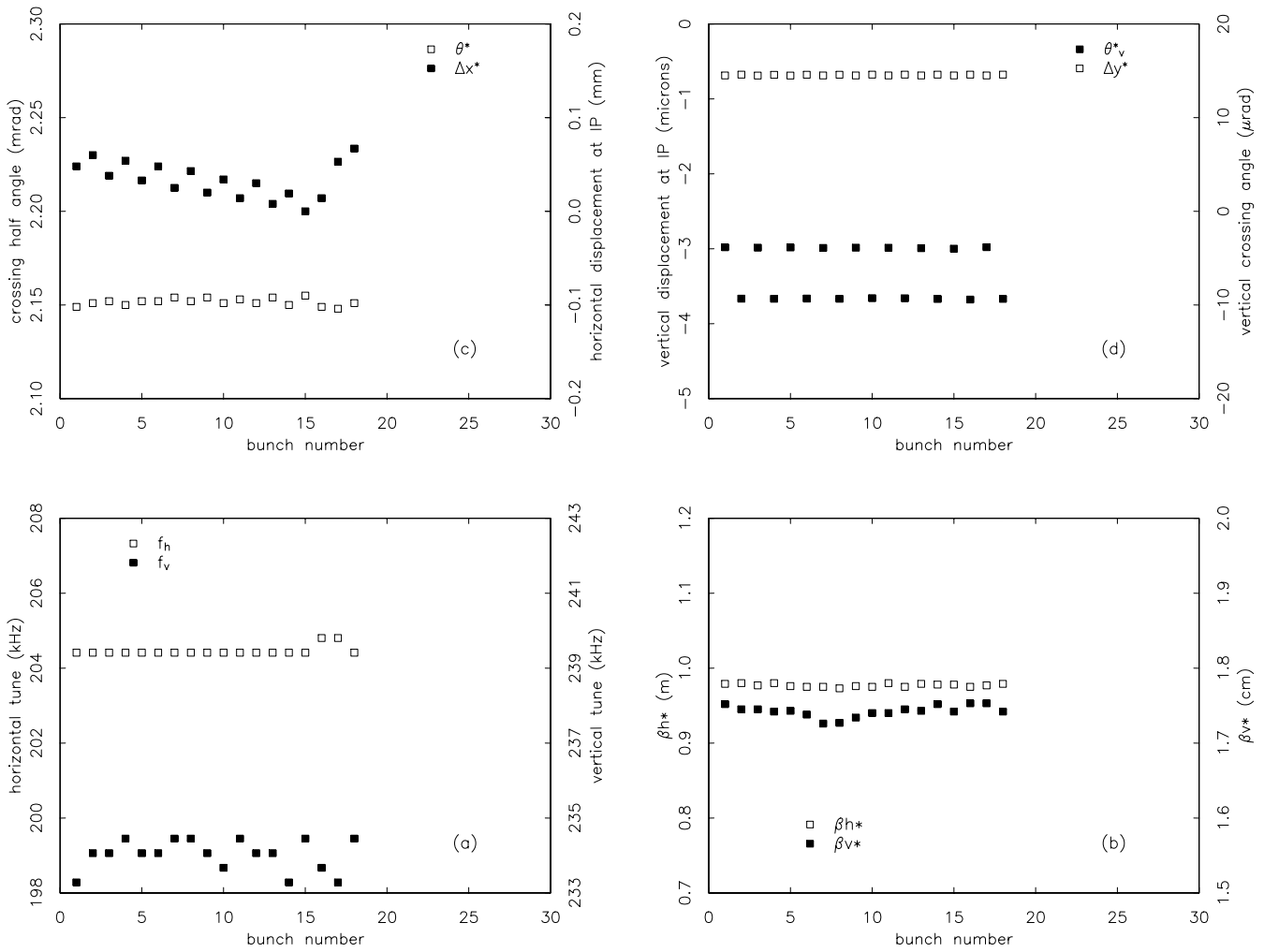

Figure 4: (a) Horizontal and vertical tune for each of 18 weak beam bunches. (b) Horizontal and vertical β^*. (c)Horizontal crossing angle and vertical separation at the IP. (d) Horizontal and vertical chromaticity bunches.

that the vertical tune is different for each and every bunch. The pattern reflects the much larger 324ns spacing between trains 9 and 1 as compared to 280ns spacing between all the other sets of trains. Bunch dependence of β_h^* is somewhat greater than that of β_v^* but the variation is small in both cases. (See Figure 3(b).)

Figures 4(c) and (d) indicates the horizontal displacement and angle of the weak beam at the interaction point. The difference in horizontal displacement is nearly 0.1mm for bunch 15 as compared to bunch 18. The bunch to bunch variation in closed orbit at the IP corresponds to an imperfect overlap of counterrotating bunches. Keep in mind that the bunches in the two beams are displaced in the opposite directions. If for example, the separators are tuned so that bunch 15 overlaps its counterpart exactly then the centers of bunches 18 will be separated by about $0.2mm$ or $\sim \frac{1}{2}\sigma_x$.

There is also a $\sim 6\mu rad$ difference in the vertical crossing angle of the bunches in each train (Figure 4(d)). The effect of crossing angle on beam-beam dynamics is characterized in terms of the "badness" parameter $\kappa = \frac{\theta_x^*}{(\sigma_x/\sigma_l)}$. For a horizontal crossing angle of $\pm 2.5mrad$, horizontal beam size of $0.4mm$ and bunch length of $2cm$, $\kappa_x \sim 0.13$. The vertical "badness" $\kappa_v \sim 0.02$ for a vertical crossing angle of $6\mu rad$ and vertical beam size of $6\mu m$. We find that the variation in vertical "badness" is very small compared to the horizontal.

The current and bunch dependence of optical functions in the Phase II on resonance optics n9a18a900.fd93s_4s with 9 3-bunch trains is shown in Figure 5 and Figure 6. The trains are distributed according to the "even" Phase II spacing. The bunches within each train are 28ns apart and the beam-beam kicks are based on the line charge approximation. The number of parasitic crossings is increased (as compared to 9X2) from 35 to 53, but because of the more nearly "even" train spacing and reconfigured IR optics, the current dependence and bunch to bunch variation of the tunes has not significantly increased. Variation in both horizontal and vertical β^* are now at the few percent level. There is about a $1kHz$ spread in horizontal tune and $2kHz$ spread in vertical tune. Variation in horizontal displacement at the IP is again close to $0.1mm$.

Figure 7 and Figure 8 show the change in closed orbit and β-function through the arcs of the machine corresponding to the Phase II 9X3 conditions of Figures 5 and 6. The change in the vertical closed orbit is less than $10\mu m$ and almost certainly negligible. The horizontal orbit has a $2mm$ peak

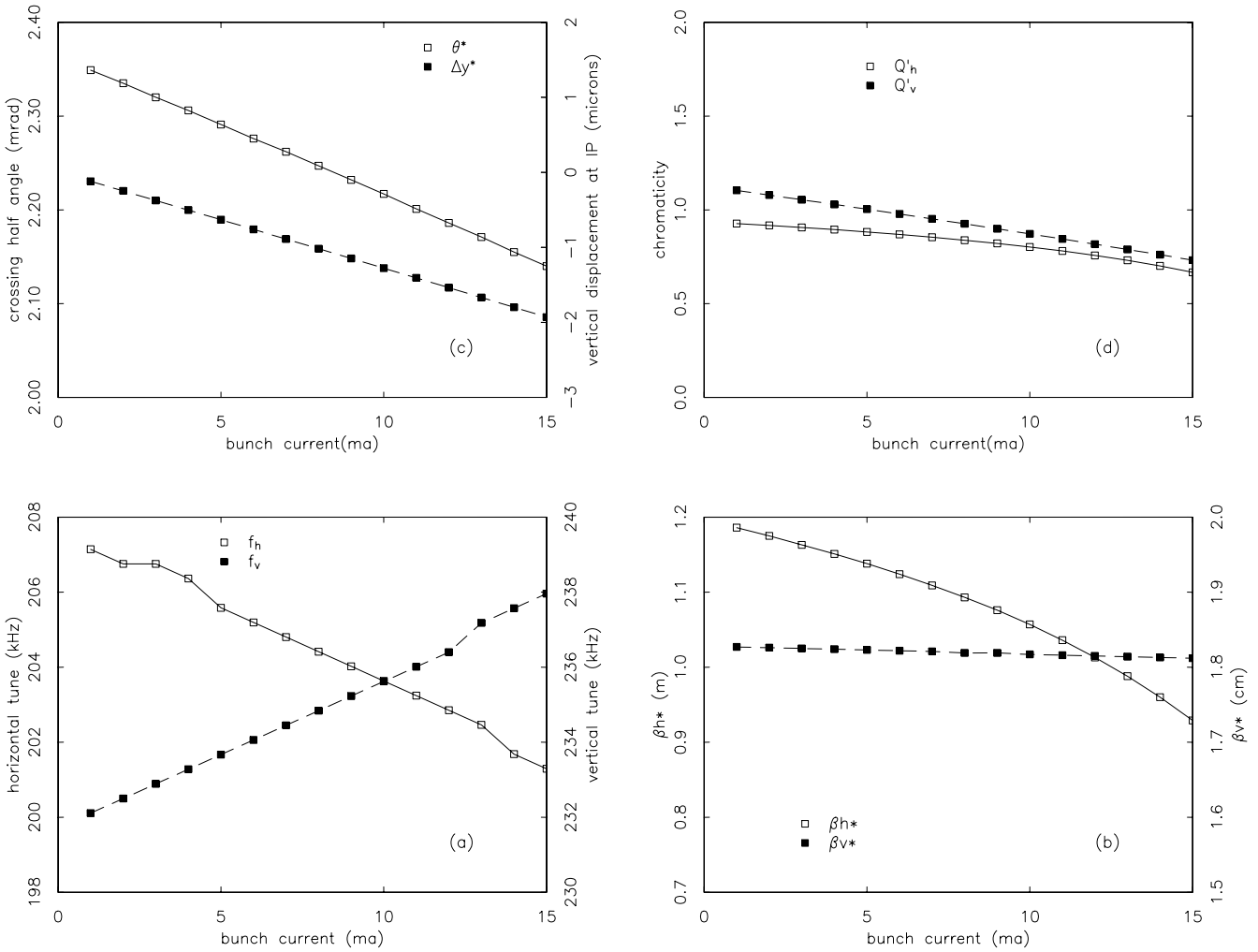

Figure 5: (a) Horizontal and vertical tune of weak beam bunch #1 as a function of bunch current in 27 bunches of positrons. (b) Horizontal and vertical β^*. (c)Horizontal crossing angle and vertical separation at the IP. (d) Horizontal and vertical chromaticity.

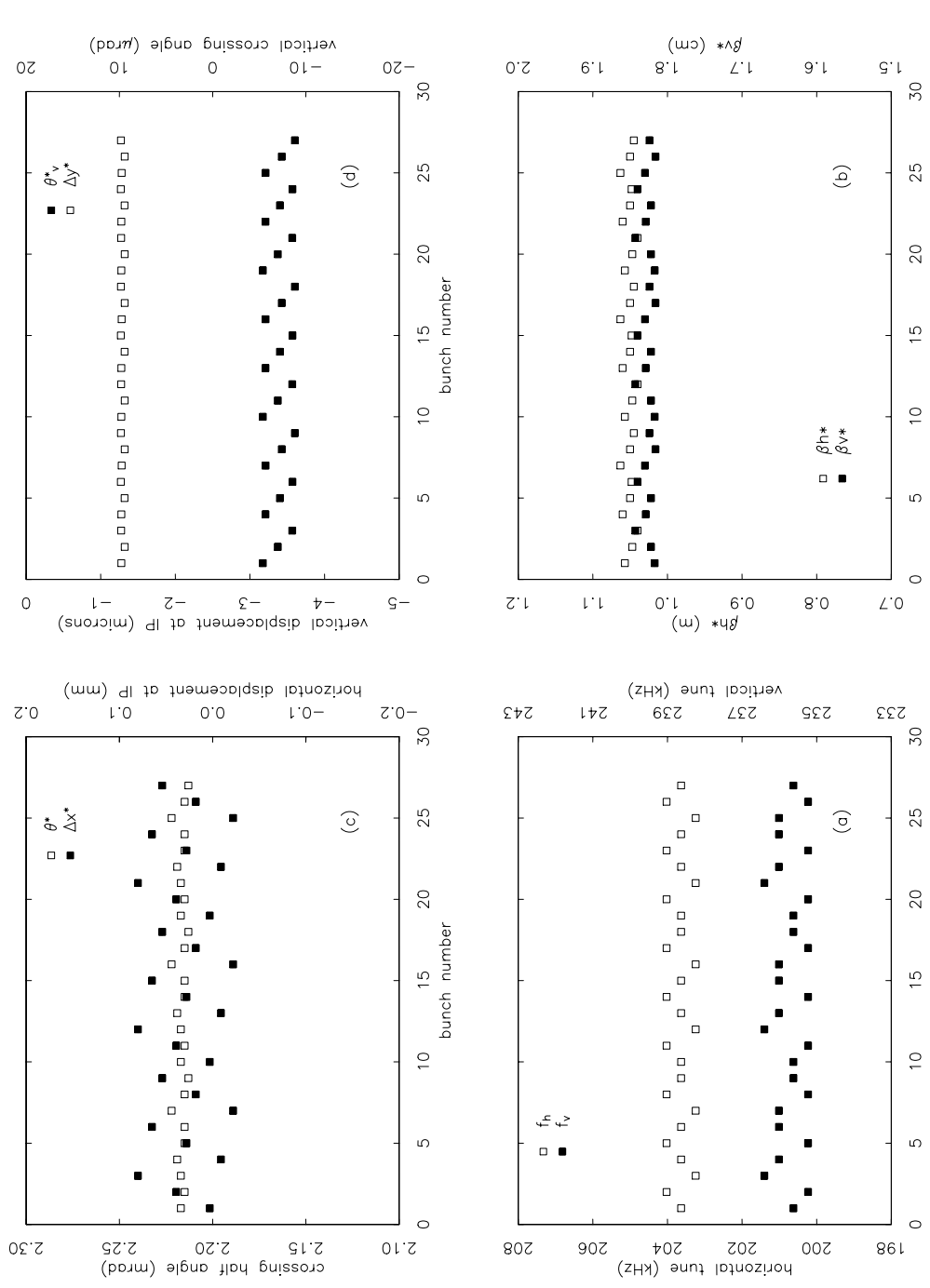

Figure 6: (a) Horizontal and vertical tune for each of 27 weak beam bunches. (b) Horizontal and vertical β^*. (c)Horizontal crossing angle and vertical separation at the IP. (d) Horizontal and vertical chromaticity.

distortion. The zero current closed orbit peak displacement is about $20mm$ so the current dependent change amounts to 10%. The distortion of the β functions through the arcs is quite significant, and vertical and horizontal comparable and at about twice the level that we typically can correct the zero current optics.

In order to assess the effectiveness of the line charge approximation of the long range interaction, the bunch dependence of optical functions are recomputed with a beam-beam kick based on the generalized 2-dimensional charge distribution. The nine 3-bunch trains of positrons are distributed according to the Phase II train spacing in the optics n9a18a900.fd93s_4s. Bunches within the trains are spaced 28ns apart. The results are shown in Figure 9. As in Figure 6 the trains are distributed according to the "even" Phase II spacing and the bunches within each train are 28ns apart. The differences are slight.

We also explore the effect of reducing the length of the 3-bunch train by spacing the bunches within each train by 14ns. The machine lattice and pretzeled orbits are the same as for the Phase II conditions described previously. The trains are distributed according to the "even" Phase II spacing and the bunches within each train are 14ns apart. The beam-beam kicks are based on the line charge approximation. The current and bunch dependence of optical functions for the case of 14ns spacing is shown in Figure 10 and Figure 11. The most significant difference in the 14ns and 28ns 3-bunch/train results is with respect to angles and displacements at the IP. The bunch to bunch variation in horizontal displacement at the IP that was on the order of $0.1mm$ in the case of 28ns spacing is reduce to $\sim 0.03mm$ for the 14ns spacing. We therefore anticipate more effective overlap of the counterrotating beams

The variation in vertical crossing angle is much greater for the more closely spaced bunches to about $20\mu rad$ or $\kappa_v \sim 0.07$. The variation in vertical angle as noted above is due to the parasitic crossings where the bunches are vertically separated. If the horizontal separation is much greater than the vertical separation (as is the case for the crossings to either side of L3), then the vertical kick is proportional to the vertical separation (see Equation 1). If the bunches are spaced 14ns apart, then the parasitic crossings adjacent to the L3 symmetry point occur in a region of greater vertical separation than for 28ns spacing.

Figure 12 shows the effect of increasing the vertical separator kick from $\pm$1mrad to $\pm$1.3mrad. The conditions are otherwise as for Figure 11, 9X3

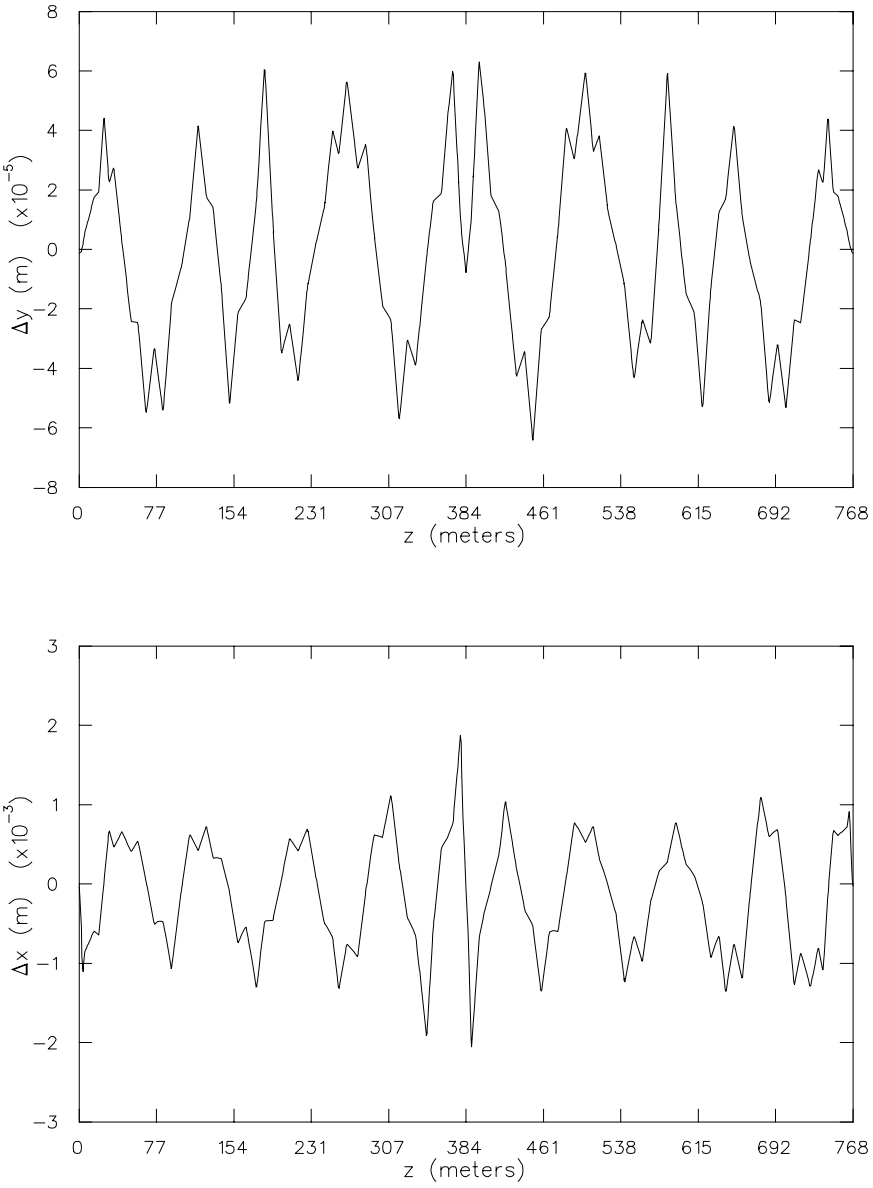

Figure 7: Change in the closed orbit of bunch #1 of the weak beam. There are 27 bunches in 9 trains in the strong beam. The bunches are spaced 28ns apart within the train and there are 10mA/bunch. The interaction point is at z=0 and 768m

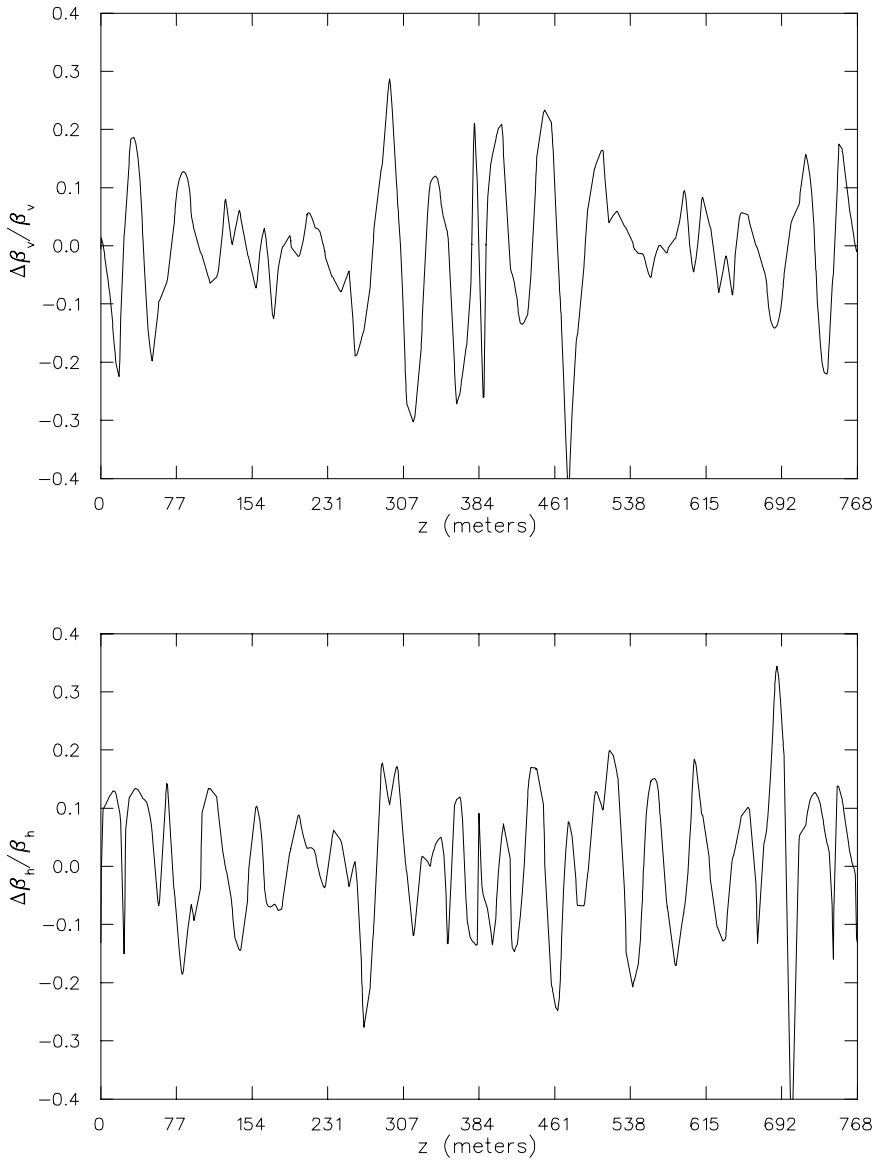

Figure 8: Fractional change in the β-function of bunch #1 of the weak beam. There are 27 bunches in 9 trains in the strong beam. The bunches are spaced 28ns apart within the train and there are 10mA/bunch. The interaction point is at z=0 and 768m

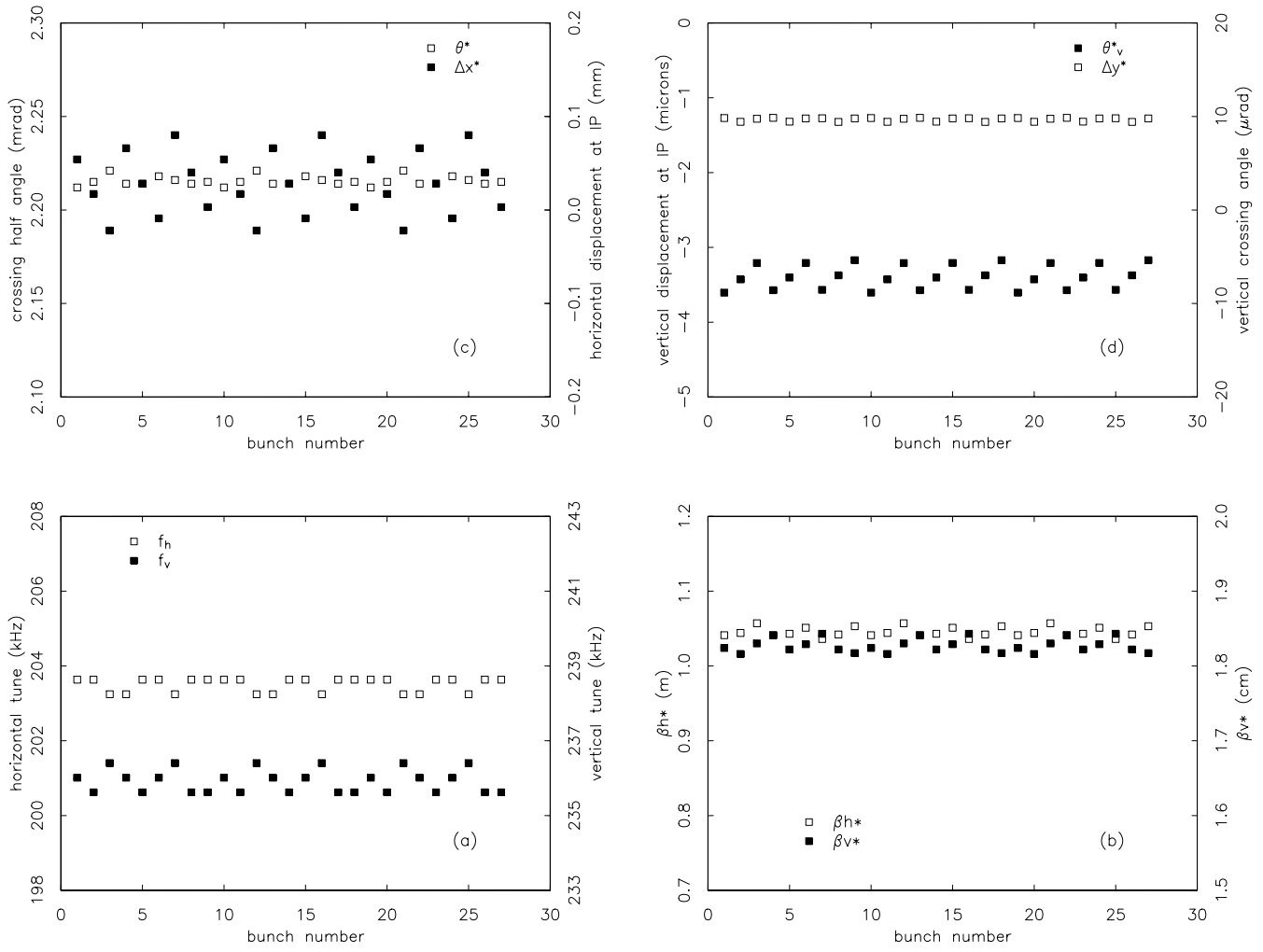

Figure 9: 9X3. Phase II train spacing. 28ns speparation within the trains. 2-dimensional beam-beam kick. Horizontal and vertical tune of weak beam bunch #1 (a) as a function of positron bunch current for 27 bunches of positrons, β^* in (b), horizontal crossing angle and horizontal displacement in (c), and vertical crossing angle and displacement in (d).

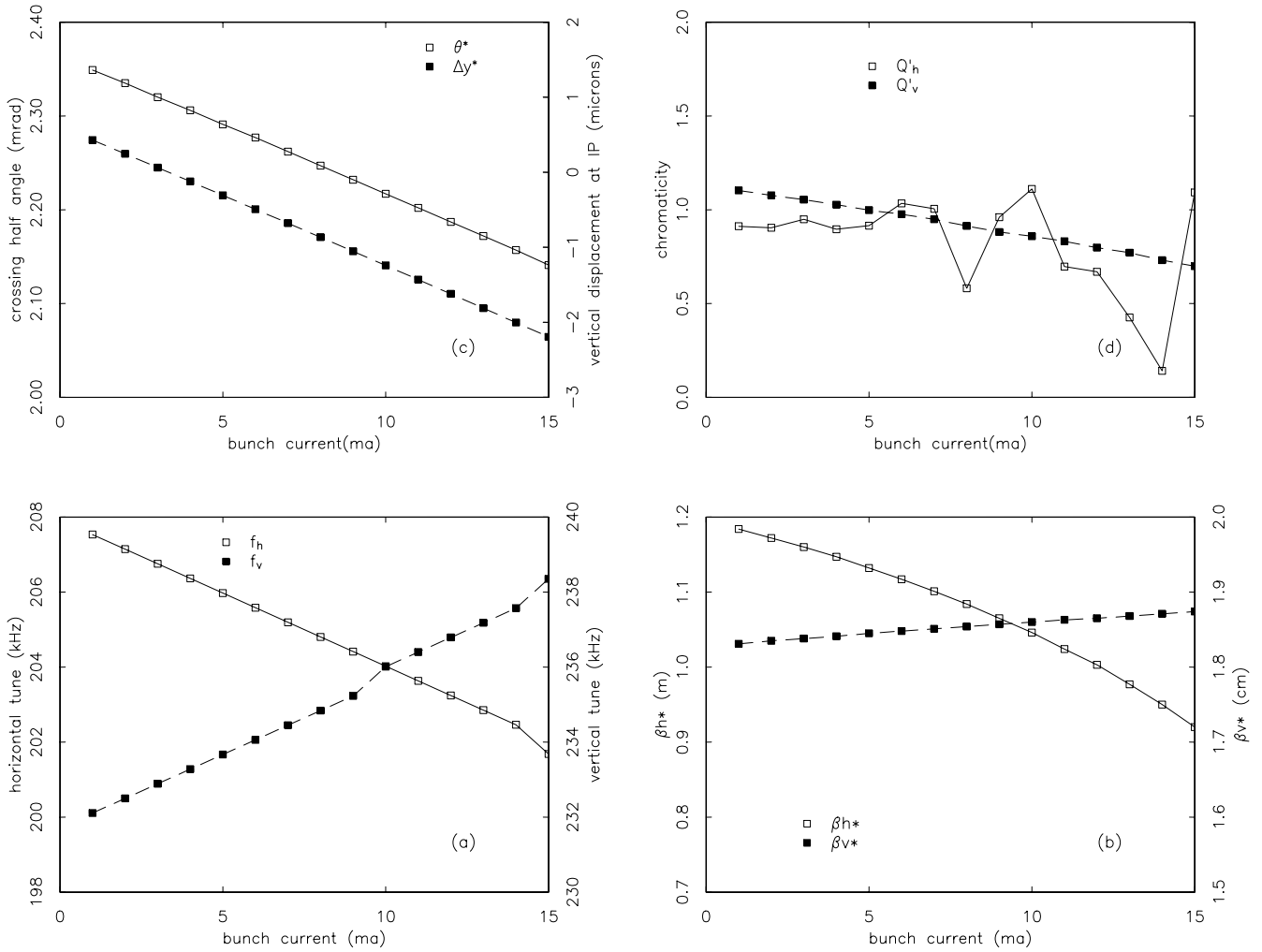

Figure 10: 9X3. Phase II even train spacing. 14ns separation within the trains. Line charge approximation of the beam-beam kicks. Horizontal and vertical tune of weak beam bunch #1 (a) as a function of positron bunch current for 27 bunches of positrons, β^* in (b), horizontal crossing angle and vertical displacement in (c), and chromaticity in (d).

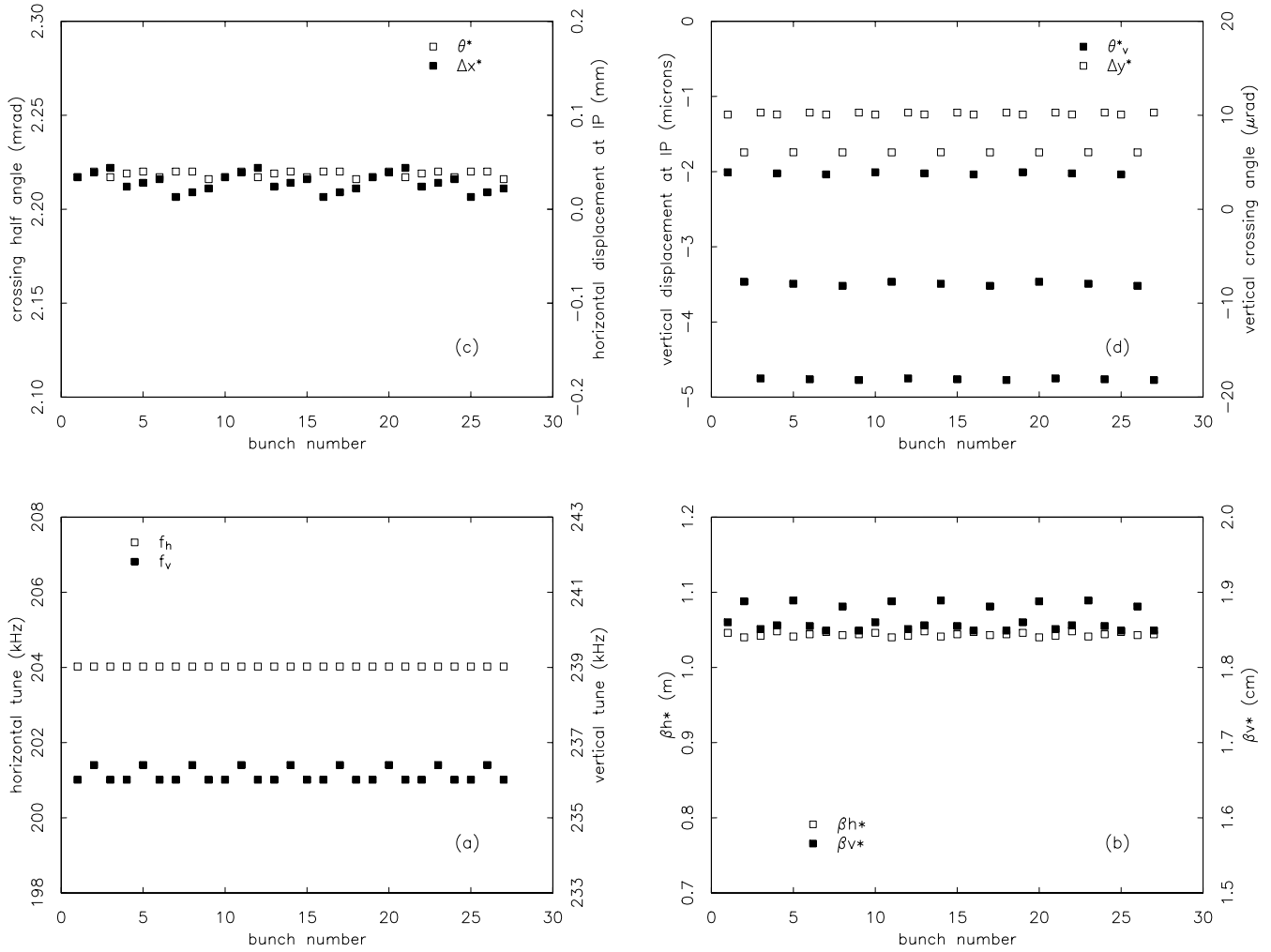

Figure 11: 9X3. Phase II even train spacing. 14ns separation of bunches within the trains. Line charge approximation of the beam-beam kicks. (a) Horizontal and vertical tune for each of 27 weak beam bunches. (b) Horizontal and vertical β^*. (c)Horizontal crossing angle and displacement the IP. (d) Vertical crossing angle and displacement.

with bunches within the trains 14ns apart.

Parasitic Interactions during electron injection

During electron injection the beams are separated horizontally at the interaction point by adding a symmetric voltage to the separators at 8E and 8W. The intersection of the closed orbits shifts to the west, so that the horizontal separation of the bunches at the parasitic crossings 2.1m and 4.2m to the west of the IP is decreased. The orbits of electron and positron beams during injection and luminosity conditions are shown in Figure 13. β_v 2.1m from the IP is 80.6m in the Phase II optics, and the effective long range tune shift is greater at the 2.1m crossing than for any other parasitic crossing in the ring. As the separation at the IP is increased, so is the tune shift due to the 2.1m crossing in the west. The optical parameters are summarized below for the parasitic crossings in the interaction region with 3-bunch trains and 14ns spacing. Injection separation corresponds to PRETZING13=-1000units.

	West 2	West 1	IP	East 1	East 2
Distance to IP (m)	4.2	2.1	0	2.1	4.2
Separation (mm)	24	10.8	2.2	19.8	40
Separation/σ_x	7.2	6.4	4.4	12.0	11.8
β_x(m)	56.6	13.8	1.2	13.8	56.6
β_y(m)	30.8	80.6	0.018	80.6	30.8
ΔQ_x	7.0(-4)	8.4(-4)	1.8(-3)	2.5(-4)	2.5(-4)
ΔQ_y	3.8(-4)	4.9(-3)	2.8(-5)	1.5(-3)	1.4(-4)

Table 1: Injection parameters for parsitic crossings near the IP

	e^- #1	e^- #2	e^- #3	e^+ #1	e^+ #2	e^+ #3
$\Sigma\Delta Q_x$	5.0(-4)	10.9(-4)	15.4(-4)	15.4(-4)	10.9(-4)	5.0(-4)
$\Sigma\Delta Q_y$	1.6(-3)	6.4(-3)	5.3(-3)	5.3(-3)	6.4(-3)	1.6(-3)

Table 2: Summed tune shifts from parasitic crossings in the IR for each of the bunches in the train during injection

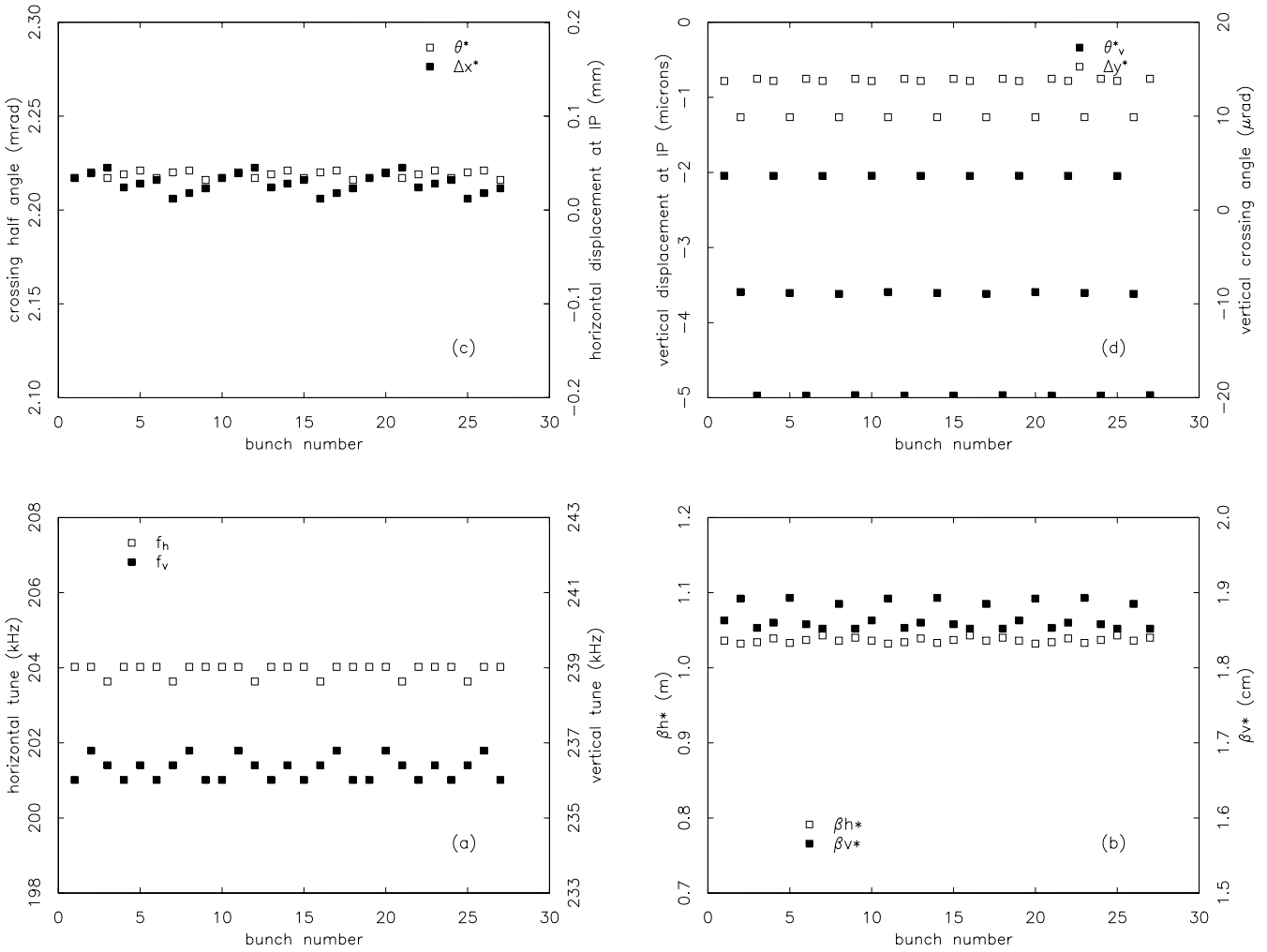

Figure 12: 9X3. Phase II even train spacing. 14ns separation of bunches within the trains. Line charge approximation of the beam-beam kicks. Vertical separator kick increased to 1.3mrad from 1.0mrad. (a) Horizontal and vertical tune for each of 27 weak beam bunches. (b) Horizontal and vertical β^*. (c)Horizontal crossing angle and displacement at the IP. (d) Vertical crossing angle and displacement.

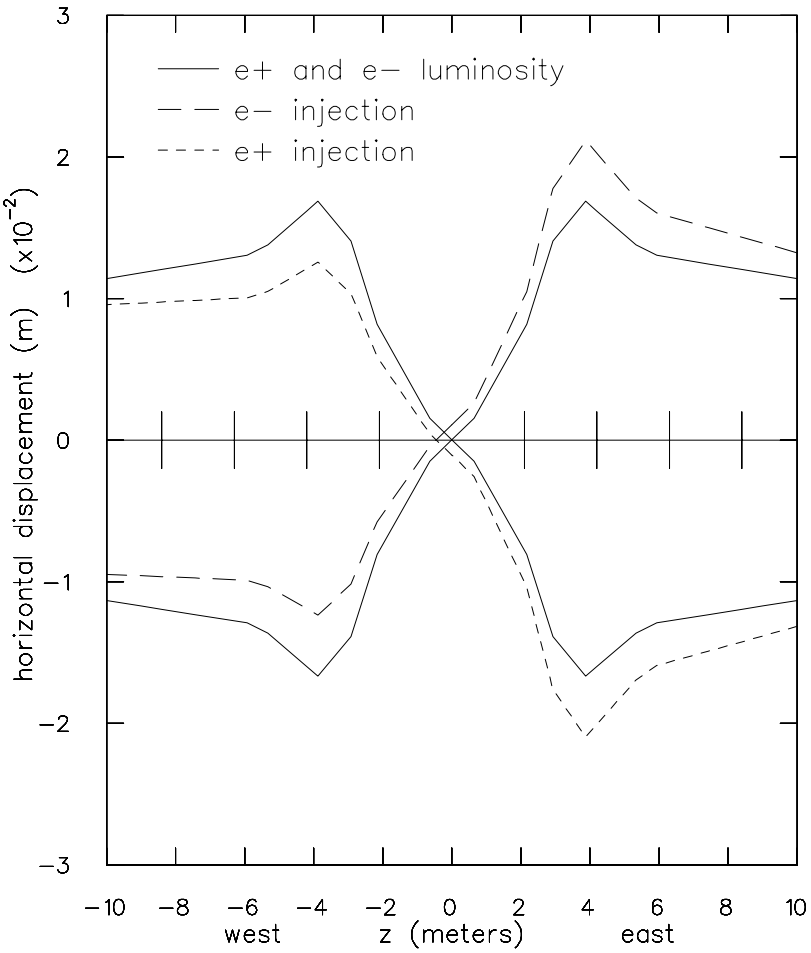

Figure 13: Solid lines indicate closed orbits of electrons and positrons colliding at the interaction point with a crossing angle. During electron injection the beams are separated at the IP by superimposing a displacement bump that extends from the separator at 8 west to the separator at 8 east. The electrons approach the IP from the northwest (lower left of the plot) and positrons approach the IP from the northeast (lower right).

Conclusions

The multiple parasitic long range interactions yield a significant current dependence to tunes, beta-functions, and closed orbits. The difference in that dependence from bunch to bunch is small except with respect to horizontal displacement at the interaction point. For trains of three bunches spaced 28ns apart, we find that the variation in horizontal displacement at the interaction point is nearly ($\pm\frac{1}{4}\sigma$), if there are 10mA/bunch in the opposing beam. If the bunches are spaced 14ns apart within the train, then the bunch to bunch differences in horizontal displacement become negligibly small. We anticipate higher average luminosity per unit current if the 3 bunches within the train are spaced 14ns apart rather than 28ns apart.